Degradation of trichloroethylene using highly adsorptive allophane–TiO_2 nanocomposite

Hiromasa Nishikiori,* Masaru Furukawa, and Tsuneo Fujii

Department of Environmental Science and Technology, Graduate School of Science and Technology, Shinshu University, 4-17-1 Wakasato, Nagano 380-8553, Japan

Corresponding author: Hiromasa Nishikiori

Tel: +81-26-269-5536

Fax: +81-26-269-5550

E-mail: nishiki@shinshu-u.ac.jp

Department of Environmental Science and Technology, Graduate School of Science and Technology, Shinshu University, 4-17-1 Wakasato, Nagano 380-8553, Japan

Abstract

A highly adsorptive allophane–TiO_2 nanocomposite photocatalyst was prepared by dispersing nanoparticles of the natural clay mineral allophane into a titanium alkoxide solution by the sol-gel method. During the photocatalytic degradation of trichloroethylene using the allophane–TiO_2 nanocomposite, emission of the intermediate product, phosgene, was drastically inhibited. Trichloroethylene was transformed into the intermediate products, phosgene and dichloroacetyl chloride, on the TiO_2 during the UV irradiation. These compounds are rapidly adsorbed on the allophane. The compounds then gradually degraded after diffusing to the TiO_2.

Keywords: Allophane; Titanium dioxide; Photocatalysis; Trichloroethylene; Adsorption

1. Introduction

Photocatalysis is a significantly important technology that is used to degrade harmful organic pollutants. On the other hand, adsorption is also a useful technique for the removal of such chemicals. Natural clay minerals have attracted considerable attention as adsorbents [1−3]. Adsorption is also important in a photocatalytic degradation process by direct hole oxidation. The clay−TiO_2 composites were studied for the effective adsorption and degradation of organic compounds [4−8]. Allophane, a natural clay mineral distributed throughout the world, is a hydrated aluminosilicate (1−2SiO_2•Al_2O_3•5−6H_2O) having a 3.5−5.0 nm-sized hollow spherical structure with 0.3−0.5 nm-sized defects on its surface [9−13]. The walls of the hollow spheres consist of inner silica and outer alumina layers with a hydroxylated or hydrated surface. Some studies suggest that these surfaces have a significant ability to adsorb ionic or polar pollutants due to their amphoteric ion-exchange activity and high surface area [9,12,14]. Allophane consists of the smallest structural units of all the clay minerals.

Trichloroethylene (TCE) is usually transformed into harmful intermediate products, such as phosgene and dichloroacetyl chloride (DCAC), during its photocatalytic degradation using TiO_2 [15−25]. It has been difficult to completely inhibit the emission of such compounds using the composites of clay mineral adsorbents and TiO_2 [6−8]. One of the reasons for this is that the particle size of the adsorbents is much larger than that of TiO_2. The inhibition of the emission of such intermediate products requires controlling the adsorption and photocatalytic reaction fields on the photocatalysts at a nanometer level in order to diffuse such compounds between the fields. The nanocomposite consisting allophane and TiO_2 is expected to effectively adsorb such compounds and degrade TCE without emitting them due to its very small particles having a high surface area. The sol−gel method is valuable for

the dispersion of small clay particles into TiO_2 by the addition of the particles into the precursor titanium alkoxide system.

In this study, the nanocomposite photocatalysts consisting of allophane and TiO_2 were prepared from the titanium alkoxide solution dispersing nanoparticles of allophane by a simple sol−gel process. The photocatalytic activity of the nanocomposite for the degradation of TCE was compared to normal TiO_2 and a mixture of allophane and TiO_2. The degradation of TCE was evaluated by FTIR spectroscopy [15,17,18,21−25].

2. Experimental

2.1. Materials

Titanium tetraisopropoxide (TTIP), hydrochloric acid (35%), TCE, and ethanol of S reagent grade were obtained from Wako Pure Chemicals. DCAC of reagent grade was obtained from Tokyo Kasei. The dry nitrogen gas and dry air gas (ca. nitrogen 79% + oxygen 21%) were obtained from Okaya Sanso. These materials were used without further purification. The water was deionized and distilled (Yamato WG23). Allophane was extracted by the elutriation of Kanuma soil from Tochigi, Japan, as already described [26−28].

2.2. Sample preparation

The sol−gel reaction systems were prepared by mixing 6.8 cm^3 of TTIP, 40.0 cm^3 of ethanol, and 1.0 cm^3 of hydrochloric acid. TTIP was dropwise added to the mixture of the other materials in a glove box filled with dry nitrogen gas at ambient temperature. The allophane was dispersed in the sol−gel system in which the Al/Ti ratio was 1/20. This ratio was selected because adding such amount of allophane clearly influenced the photocatalytic activity. The sol−gel systems with and without allophane were agitated by ultrasonication

for 3 days. The resulting gel samples were hydrothermally treated at 100°C, then heated at 400 °C for 3 h.

2.3. Characterization of samples

The prepared samples were characterized by XRD analysis using Cu Kα radiation (Rigaku RINT2000) and SEM (Hitachi S-4100). The size of the crystallites of each sample was estimated from its full-width at half-maximum of the 25.3° peak in the XRD pattern using Sherrer's equation, $D=0.9\lambda/\beta\cdot\cos\theta$. The specific surface areas of the samples were measured by the volumetric gas adsorption method using nitrogen gas (BEL Japan, BELSORP-mini).

The amounts of TCE and DCAC adsorbed on the samples were estimated by gas chromatography-mass spectrometry (Shimadzu GCMS-QP5000). DCAC is a product of the TCE degradation. Allophane of 3.0 mg or each of the other sample of 30 mg was placed in a glass vial. The TCE gas diluted with dry air was injected into the vials in which its concentration was 3.2×10^{-4} mol dm^{-3}. Allophane of 1.0 mg or each of the other sample of 10 mg was also placed in other glass vial. The DCAC gas diluted with dry air was injected into the vials in which its concentration was 3.2×10^{-4} mol dm^{-3}. The adsorption abilities of the samples for TCE and DCAC were estimated from the concentrations after their adsorption equilibria by GCMS analysis.

2.4. Photocatalytic degradation of TCE

The samples of 0.30 g were placed in an infrared cell made of Pyrex glass with KBr single crystals. The TCE gas diluted with dry air was injected into the infrared cell in which its concentration was 3.2×10^{-4} mol dm^{-3}. The cell was kept at ambient temperature until the adsorption of TCE was equilibrated. The degradation reaction of the TCE was carried out in the cell by near-UV light irradiation using a 4 W black light bulb (Toshiba FL4BLB) at ambient temperature. The FTIR spectra (Shimadzu FTIR-8300) of the gas

phase in the cell were observed as a function of the light irradiation time. The changes in the concentrations of TCE and the products were determined during the TCE degradation using the prepared TiO_2 (Sample T) and allophane−TiO_2 composite (Sample C) and the mixture of allophane and TiO_2 (Al/Ti = 1/20) (Sample M). The TCE degradation was repeated six times after each gas replacement.

The changes in the concentration of CO_2 produced from the Samples T, M, and C were observed during the UV irradiation after the fourth TCE degradation in order to examine the degradation of the species adsorbed on the samples.

3. Results and discussion

3.1. Characterization of the samples

Figure 1 shows the SEM images of Samples T and C. Sample T consisted of 20–30 nm-sized particles. Sample C contained the 5–10 nm-sized particles attributed to the allophane. The particle size of TiO_2 in Sample C was also smaller than that in Sample T because the allophane prevented the particle growth of TiO_2. The EDX analysis revealed the allophane particles were highly dispersed among the TiO_2 particles as previously shown [28].

The anatase and rutile-type crystals were observed in Sample T by XRD analysis. Their crystallite sizes were estimated using Sherrer's equation to be 8.9 nm for the anatase and 7.6 nm for the rutile. Sample C contained 7.0 nm anatase-type crystallites. The samples also consisted of secondary particles. The secondary particles of Sample C should consist of the allophane and TiO_2 nanoparticles.

The specific surface areas of the allophane and Samples T, M, and C were estimated to be 312, 66.0, 90.6, and 95.1 m^2g^{-1}, respectively. The value of the allophane was much greater

than that of the TiO_2. The values of Samples M and C correspond to the sum of the fractional specific surface areas of the allophane and TiO_2.

(Figure 1)

3.2. Photocatalytic degradation of TCE

The concentration of TCE decreased while those of CO and CO_2 increased due to the UV irradiation during the first photocatalytic degradation of TCE for all the samples. The expected products, phosgene, DCAC, and HCl, were not found in the first run due to adsorption by the TiO_2 or allophane [29]. TCE was not detected after the 20-min irradiation using Samples T and M, and after the 360-min irradiation using Sample C. Phosgene and HCl were detected after the first run using Sample T, and after the second run using Samples M and C. DCAC was detected after the first run using Samples T and M, and after the third run using Sample C.

The specific surface areas and adsorption capacities of the allophane and Samples T, M, and C for TCE and DCAC were shown in Table 1 with their crystallite sizes. The amounts of TCE and DCAC adsorbed on the samples depend on the surface area. The amounts of TCE adsorbed by Samples T, M, and C were 13, 21, and 18% of the initial amount of TCE provided for the photocatalytic degradation, respectively. The adsorption capacity for DCAC, especially of the allophane, was much greater than that for TCE due to its preference of hydrophilic surface. The amount of DCAC adsorbed on Sample T was three times greater than the initial amount of TCE. It is reported that TiO_2 can adsorb DCAC to some extent [17−19,24,29]. The adsorption capacities of Samples M and C for DCAC are about four times greater than that of Sample T.

(Table 1)

Figure 2 shows the changes in the concentrations of TCE and the products from the third TCE degradation during UV irradiation using Samples T, M, and C. The TCE decreased

and disappeared after the 10-min irradiation of Samples T and M, and after the 45-min irradiation of Sample C. The degradation rate of TCE using Sample C was much slower than for the other two samples. Compared to Sample T, Samples M and C emit fewer chlorine compounds due to their adsorption. The maximum concentrations of the emitted phosgene for Samples M and C were 1/10 and 1/20 of those for Sample T. DCAC and HCl were detected at around the time when the TCE disappeared.

(Figure 2)

TCE was transformed into the intermediate products, phosgene and DCAC, on the TiO_2 during the UV irradiation [15−25]. Most of the TCE was transformed into phosgene during the third run using Sample T. The concentration of phosgene in the final stage of the run, 4.4×10^{-4} mol dm^{-3}, indicated that phosgene was also produced from the species adsorbed during the first and second runs. Phosgene and DCAC are rapidly adsorbed on the allophane in Samples M and C [29]. The compounds were gradually degraded after diffusing to the TiO_2. The evolution of CO and CO_2 also gradually progressed, whereas the concentrations were much lower than that of the provided TCE. Most of the intermediate products, phosgene and DCAC, should be adsorbed on the allophane even during the final stage of the runs. The allophane particles in Sample C exhibited a high adsorption efficiency due to their high dispersion even though it inhibited the degradation performance by acting as an inner light filter.

3.3. Degradation process of TCE

Figure 3 shows the changes in the average degradation rate of TCE during the repeated runs using Samples T, M, and C. The degradation rate increased with the repeated run for all the samples. Such phenomenon was observed in the case using the catalysts prepared at low temperature [30,31]. This suggests that the TiO_2 was activated by decreasing the oxygen defects or impurities on the surface during the UV irradiation. The Cl radical

emitted from the chlorine compounds adsorbed on the samples also promoted the TCE degradation [32].

(Figure 3)

Figure 4 shows the changes in the integrated concentration of phosgene produced during the repeated runs using Samples T, M, and C. A very small amount of phosgene was detected before the third run using all the samples due to the adsorption of the intermediate products, mainly DCAC. These compounds were detected after reaching the adsorption saturation. Based on the amount of the produced phosgene, almost all of the provided TCE was finally transformed into phosgene during the photocatalytic degradation of TCE using Sample T. This is because a greater amount of the adsorption species, such as DCAC, was transformed into phosgene in the latter run by the UV activation of TiO_2 [29,33]. Most of the produced phosgene was emitted from the Sample T surface into the gas phase. TiO_2 and even allophane are expected to much less adsorb phosgene than DCAC because they can adsorb the amounts of DCAC equivalent to those of TCE provided for the three and twelve times TCE degradation, respectively.

(Figure 4)

The TCE degradation rate using Sample T was almost the same as that using Sample M as shown in Fig. 3. This indicates that their activities and phosgene-production rates are almost the same. However, the phosgene concentration observed after the TCE degradation using Samples T was different from that using Sample M due to the difference in their phosgene adsorption abilities. Almost all of the TCE was transformed into phosgene after the third degradation using Sample T. The adsorption abilities of Samples M and C are expected to be nearly the same amount of TCE provided for the four times degradation. The difference in the phosgene concentration observed between using Samples M and C reflects those in the photocatalytic activity and the amount of the produced phosgene.

3.4. Reaction of the adsorbed species

Most of the produced phosgene and DCAC should be adsorbed on Samples M and C after the TCE degradation. Figure 5 shows the change in the concentration of CO_2 produced from Samples T, M, and C during the UV irradiation after the fourth TCE degradation. CO_2 was gradually produced from Samples M and C even though no phosgene was detected. The degradation rate was very slow since ca. 2% of the adsorbed phosgene and DCAC molecules were degraded to CO_2 for 20 h. However, the concentration of CO_2 produced from Sample C was three times greater than that from Sample M by degradation of the adsorbed phosgene and DCAC. Furthermore, the amount of CO_2 produced from Sample C increased to ca. 10% of the adsorbed species after 240-h irradiation. This value is ten times larger than in that from Sample M. The difference in the CO_2 production rate reflects the difference in the rate of the surface diffusion of phosgene from the allophane to the TiO_2. The diffusion rate on Sample C is faster than on Sample M due to high dispersion of allophane into the TiO_2. On the other hand, phosgene in the gas phase was mainly degraded during the TCE degradation using Sample T.

(Figure 5)

4. Conclusions

A highly adsorptive allophane–TiO_2 nanocomposite photocatalyst was prepared by dispersing nanoparticles of the natural clay mineral allophane into a titanium alkoxide solution by the sol-gel method. The photocatalytic activity of the nanocomposite for the degradation of TCE was compared to the normal TiO_2 and the allophane–TiO_2 mixture. The photocatalytic degradation of TCE using the allophane-containing TiO_2, especially the nanocomposite, drastically inhibited the emission of the intermediate product, phosgene.

TCE was transformed into the intermediate products, phosgene and dichloroacetyl chloride, on the TiO_2 during the UV irradiation. These compounds are rapidly adsorbed on the allophane. The compounds then gradually degraded after diffusing to the TiO_2. The diffusion rate on the nanocomposite was faster than on the mixture due to high dispersion of allophane into the TiO_2. The allophane in the nanocomposite plays an important role in the adsorption of the intermediate species and the mediation of them between the gas phase and the TiO_2 surface.

Acknowledgement

The authors thank Dr. T. Matsumoto of the Tochigi Research Institute for kindly providing the allophane.

References

[1] S. Xu, R.G. Lehmann, J.R. Miller, G. Chandra, Environ. Sci. Technol. 32 (1998) 1199−1206.

[2] F. Bergaya, K.G. Theng, G. Lagaly, Handbook of clay science, Elsevier, Amsterdam 2006.

[3] M. Cea, J.C. Seaman, A.A. Jara, B. Fuentes, M.L. Mora, M.C. Diez, Chemosphere 67 (2007) 1354−1360.

[4] H. Yoneyama, S. Haga, and S. Yamanaka, J. Phys. Chem. 93 (1989) 4833−4837.

[5] Y. Kitayama, T. Kodama, M. Abe, and H. Shimotsuma, J. Porous Mater. 5 (1998) 121−126.

[6] T. Tao, J. J. Yang, G. E. Maciel, Environ. Sci. Technol. 33 (1999) 74−80.

[7] S. Suárez, J. M. Coronado, R. Portela, J. C. Martín, M. Yates, P. Avila, B. Sánchez, Environ. Sci. Technol. 42 (2008) 5892−5896.

[8] T. L. R. Hewer, S. Suárez, J. M. Coronado, R. Portela, P. Avila, B. Sánchez, Catal. Today 143 (2009) 302−308.

[9] Y. Kitagawa, Am. Mineralogist 56 (1971) 465−475.

[10] T. Henmi, K. Wada, Am. Mineralogist 61 (1976) 379−390.

[11] S. Wada, K. Wada, Clay Miner. 12 (1977) 289−298.

[12] P.L. Hall, G.J. Churkman, B.K.G. Theng, Clays Clay Miner. 33 (1985) 345−349.

[13] S.J. van der Gaast, K. Wada, S.-I Wada, Y., Kakuto, Clays Clay Miner. 33 (1985) 237−243.

[14] E. Hanudin, N. Matsue, T. Henmi, Clay Sci. 11 (1999) 57−72.

[15] W. A. Jacoby, M. R. Nimlos, D. M. Blake, R. D. Noble, C. A. Koval, Environ Sci. Technol. 28 (1994) 1661−1668.

[16] S. Yamazaki-Nishida, S. Cervera-March, K. J. Nagano, M. A. Anderson, K. Hori, J. Phys. Chem. 99 (1995) 15814−15821.

[17] J. Fan, J. T. Yates, Jr., J. Am. Chem. Soc. 118 (1996) 4686−4692.

[18] M. D. Driessen, A. L. Goodman, T. M. Miller, G. A. Zaharias, V. V. Grassian, J. Phys. Chem. B 102 (1998) 549−556.

[19] S. J. Hwang, C. Petucci, D. Raftery, J. Am. Chem. Soc. 120 (1998) 4388−4397.

[20] K. H. Wang, H. H. Tsai, Y. H. Hsieh, Appl. Catal. B: Environ. 17 (1998) 313−320.

[21] J. S. Kim, K. Itoh, M. Murabayashi, Chemosphere 36 (1998) 483−495

[22] P. B. Amama, K. Itoh, M. Murabayashi, J. Mol. Catal. A: Chem. 176 (2001) 165−172.

[23] K. Oki, S. Tsuchida, H. Nishikiori, N. Tanaka, T. Fujii, Int. J. Photoenergy 5 (2003) 11−15.

[24] S. K. Joung, T. Amemiya, M. Murabayashi, K. Itoh, Chem. Eur. J. 12 (2006) 5526−5534.

[25] Y. Yokosuka, K. Oki, H. Nishikiori, Y. Tatsumi, N. Tanaka, T. Fujii, Res. Chem. Intermed. 35 (2009) 43−53.

[26] H. Nishikiori, J. Shindoh, N. Takahashi, T. Takagi, N. Tanaka, T. Fujii, Appl. Clay Sci. 43 (2009) 160−163.

[27] H. Nishikiori, K. Kobayashi, S. Kubota, N. Tanaka, T. Fujii, Appl. Clay Sci. 47 (2010) 325−329.

[28] H. Nishikiori, M. Furukawa, S. Ichihashi, J. Environ. Chem. 20 (2010) 371−377.

[29] S. K. Joung, T. Amemiya, M. Murabayashi, K. Itoh, J. Photochem. Photobiol. A: Chem. 184 (2006) 273−281.

[30] M. Asiltürk, F. Sayılkan, S. Erdemoğlu, M. Akarsu, H. Sayılkan, M. Erdemoğlu, E. Arpaç, J. Hazardous Mater. B129 (2006) 164−170.

[31] F. Sayılkan, S. Erdemoğlu, M. Asiltürk, M. Akarsu, Ş. Şener, H. Sayılkan, M. Erdemoğlu, E. Arpaç, Mater. Res. Bull. 41 (2006) 2276−2285.

[32] M. Murabayashi, K. Itoh, Z. L. Hua, K. Kitahara, J. Adv. Oxidation Technol. 5 (2002) 67−71.

[33] A. C. Lukaski, D. S. Muggli, Catal. Lett. 89 (2003) 129−138.

Table 1 Characteristics of allophane and Samples T, M, and C.

	allophane	Sample T	Sample M	Sample C
crystallite size / nm	-	8.9 (anatase) 7.6 (rutile)	8.9 (anatase) 7.6 (rutile)	7.0 (anatase)
specific surface area / m^2g^{-1}	312	66.0	90.6	95.1
TCE adsorption capacities / 10^{-5} mol g^{-1}	26.3	1.42	2.20	1.92
DCAC adsorption capacities / 10^{-5} mol g^{-1}	>1000	30.7	126	133

Figure captions

Figure 1. SEM images of (a) Sample T and (b) Sample C.

Figure 2. Changes in the concentrations of TCE and the products from the third TCE degradation during the UV irradiation using (a) Sample T, (b) Sample M, and (c) Sample C. The factors of the concentrations of phosgene are (a) 0.2, (b) 2, and (c) 2.

Figure 3. Change in the average degradation rate of TCE during the repeated TCE degradation using (1) Sample T, (2) Sample M, and (3) Sample C.

Figure 4. Change in the integrated concentration of phosgene produced during the repeated TCE degradation using (1) Sample T, (2) Sample M, and (3) Sample C.

Figure 5. Change in the concentration of CO_2 produced from (1) Sample T, (2) Sample M, and (3) Sample C during the UV irradiation after the fourth TCE degradation. The time ranges are (a) 0−1300 min and (b) 0−250 h.

Figure 1

(a)

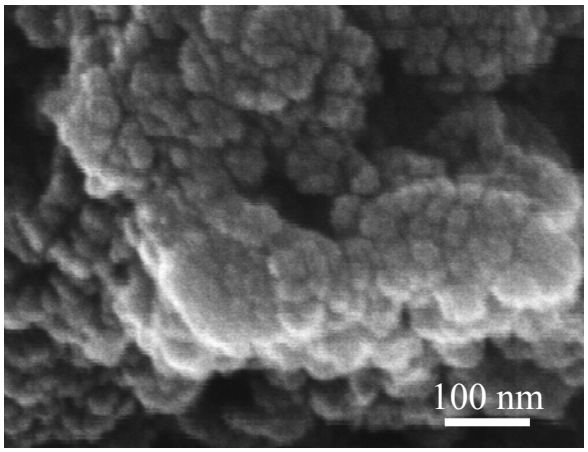

(b)

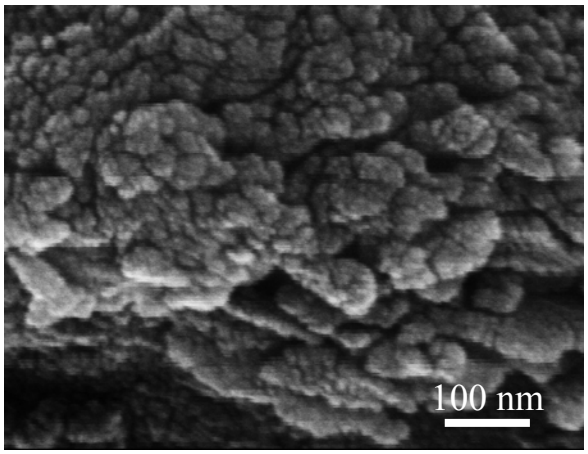

Figure 2

(a)

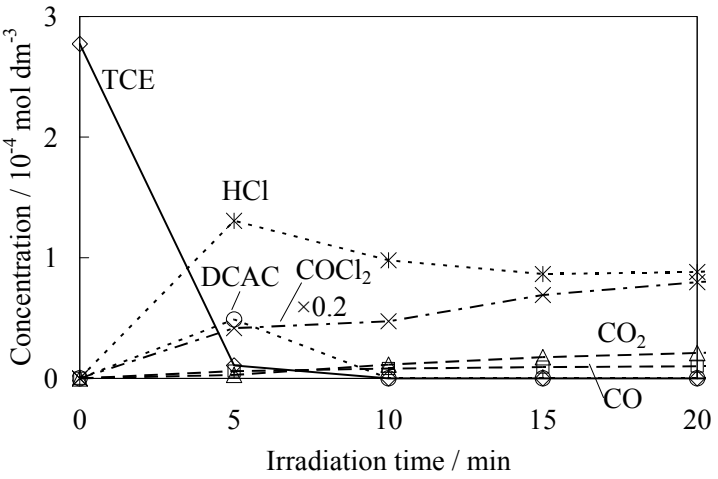
Concentration / 10^{-4} mol dm^{-3}
Irradiation time / min
TCE
HCl
DCAC
$COCl_2$ ×0.2
CO_2
CO

(b)

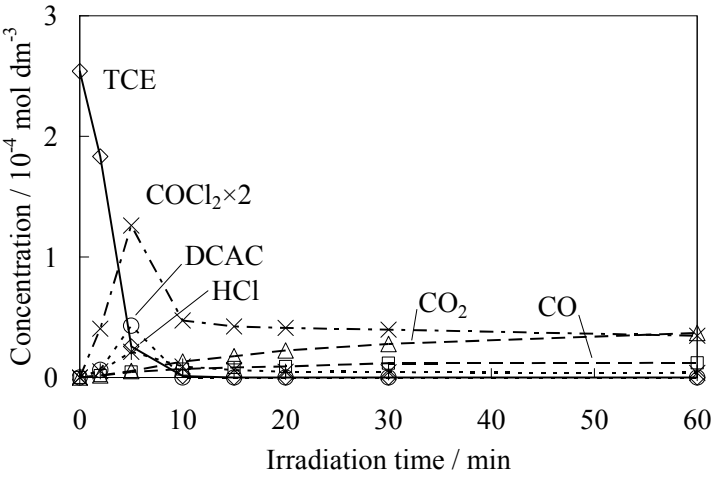
Concentration / 10^{-4} mol dm^{-3}
Irradiation time / min
TCE
$COCl_2$×2
DCAC
HCl
CO_2
CO

(c)

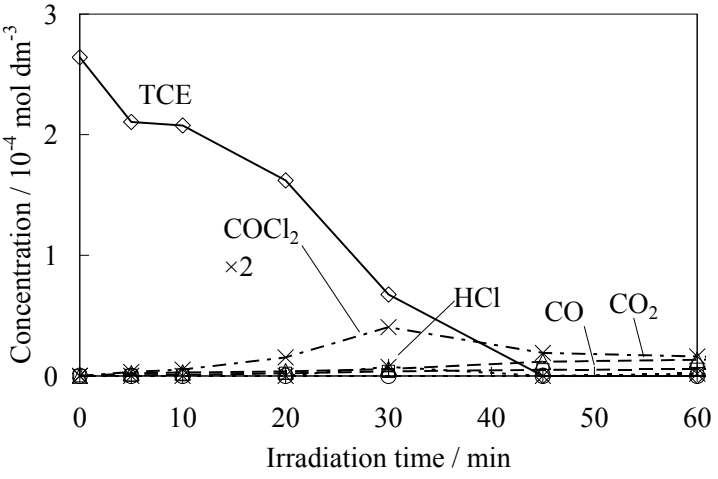
Concentration / 10^{-4} mol dm^{-3}
Irradiation time / min
TCE
$COCl_2$ ×2
HCl
CO
CO_2

Figure 3

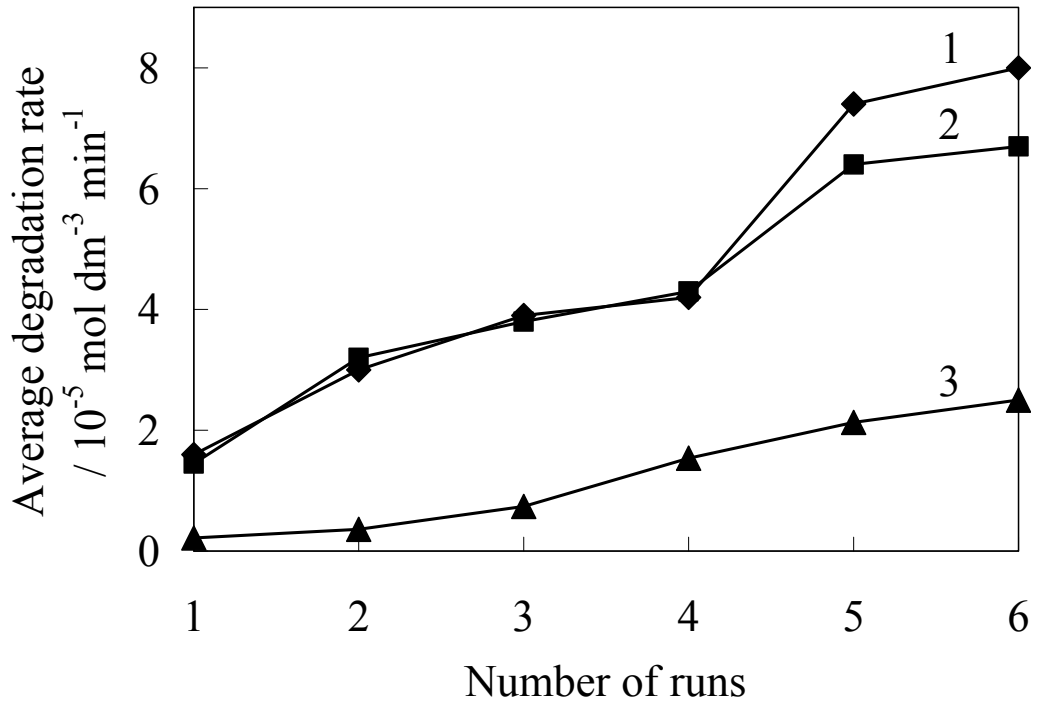
Average degradation rate
/ 10-5 mol dm-3 min-1
0
2
4
6
8
1
2
3
4
5
6
Number of runs
1
2
3

Figure 4

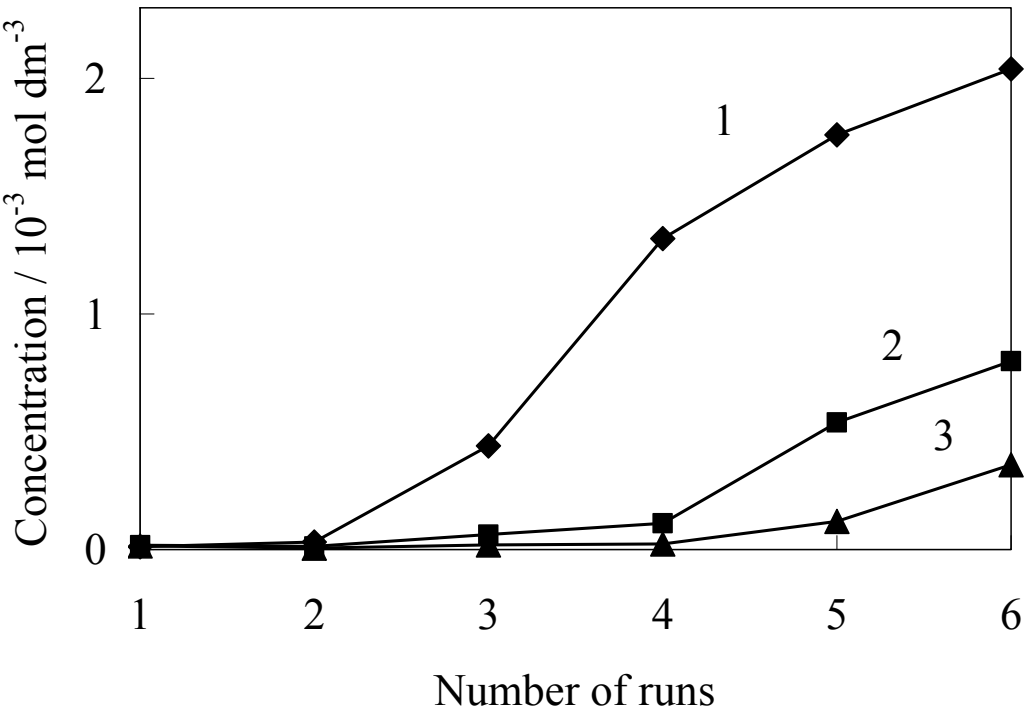

Figure 5

(a)

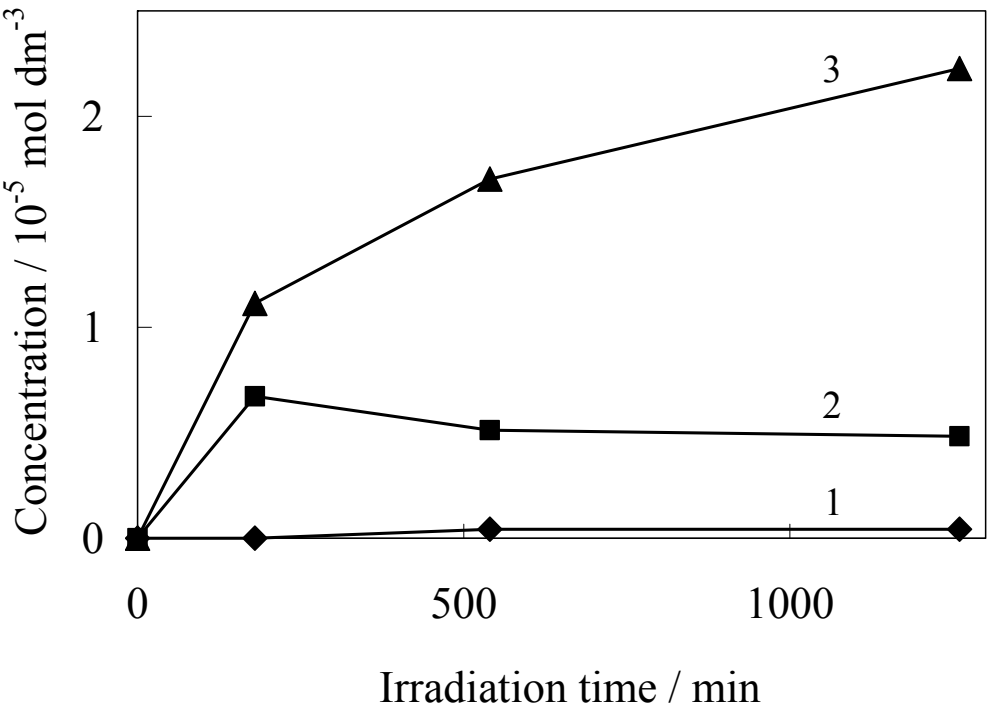
Concentration / 10-5 mol dm-3
0
1
2
3
2
1
0
500
1000
Irradiation time / min

(b)

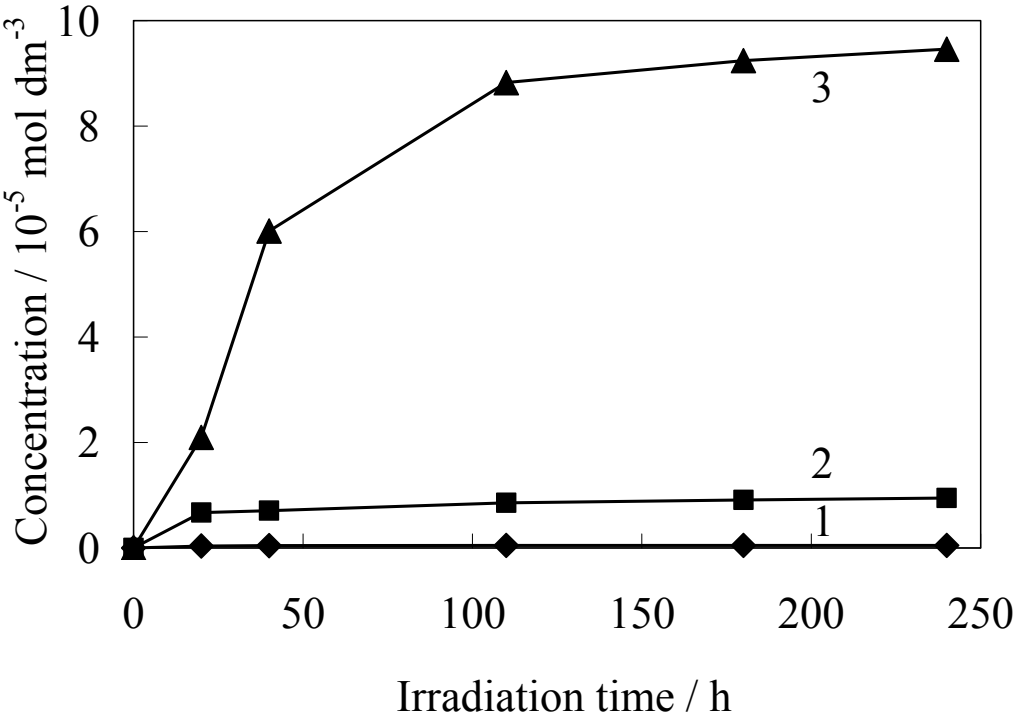
Concentration / 10-5 mol dm-3
0
2
4
6
8
10
3
2
1
0
50
100
150
200
250
Irradiation time / h